

Rescue of Monocrotaline-Induced Pulmonary Arterial Hypertension Using Bone Marrow–Derived Endothelial-Like Progenitor Cells

Efficacy of Combined Cell and eNOS Gene Therapy in Established Disease

Yidan D. Zhao, David W. Courtman, Yupu Deng, Lakshmi Kugathasan, Qiuwang Zhang, Duncan J. Stewart

Abstract—Pulmonary arterial hypertension (PAH) is characterized by a progressive increase in pulmonary vascular resistance caused by narrowing and loss of pulmonary microvasculature, which in its late stages becomes refractory to traditional therapies. We hypothesized that bone marrow–derived endothelial progenitor cells (EPCs), which normally function to repair and regenerate blood vessels, would restore pulmonary hemodynamics and increase microvascular perfusion in the rat monocrotaline (MCT) model of PAH. Mononuclear cells were isolated from the bone marrow of syngeneic Fisher-344 rats by Ficoll gradient centrifugation and cultured for 7 to 10 days in endothelial growth medium. Fluorescently labeled endothelial-like progenitor cells (ELPCs) engrafted at the level of the distal pulmonary arterioles and incorporated into the endothelial lining in the MCT-injured lung. The administration of ELPCs 3 days after MCT nearly completely prevented the increase in right ventricular systolic pressure seen at 3 weeks with MCT alone (31.5 ± 0.95 versus 48 ± 3 mm Hg, respectively; $P < 0.001$), whereas injection of skin fibroblasts had no protective effect (50.9 ± 5.4 mm Hg). Delayed administration of progenitor cells 3 weeks after MCT prevented the further progression of PAH 2 weeks later (ie, 5 weeks after MCT), whereas only animals receiving ELPCs transduced with human endothelial NO-synthase (eNOS) exhibited significant reversal of established disease at day 35 (31 ± 2 mm Hg, $P < 0.005$) compared with day 21 (50 ± 3 mm Hg). Fluorescent microangiography revealed widespread occlusion of pulmonary precapillary arterioles 3 weeks after MCT, whereas arteriolar-capillary continuity and microvascular architecture was preserved with the administration of syngeneic ELPCs. Moreover, the delivery of ELPCs to rats with established PAH resulted in marked improvement in survival, which was greatest in the group receiving eNOS-transduced cells. We conclude that bone marrow–derived ELPCs can engraft and repair the MCT-damaged lung, restoring microvasculature structure and function. Therefore, the regeneration of lung vascular endothelium by injection of progenitor cells may represent a novel treatment paradigm for patients with PAH. (*Circ Res.* 2005;96:442-450.)

Key Words: progenitor cells ■ pulmonary hypertension ■ endothelium ■ endothelial nitric oxide synthase

Pulmonary arterial hypertension (PAH) is a devastating disease that in its most severe form, idiopathic PAH, leads to progressive debilitation and death, often within 2 to 3 years after its initial diagnosis.¹ Despite significant advances in the therapy of PAH during the last decade, the prognosis remains poor. Although the genetic basis for some patients with familial PAH has been elucidated,²⁻⁴ how these mutations are causally linked to the development of PAH remains unclear.^{5,6} Evidence from experimental models as well as lung specimens from patients with PAH underlines the importance of microvascular occlusion in the pathogenesis of this disease,⁷ especially in its advanced stages; however, the precise mechanisms remain uncertain. Recently, it

has been suggested that environmental stress in a genetically predisposed host may trigger endothelial cell apoptosis,^{8,9} which could lead to arteriolar occlusion either directly, possibly by initiating microvascular degeneration,¹⁰ or indirectly by promoting the emergence of hyperproliferative, apoptosis-resistant endothelial clones.^{11,12} Regardless of the mechanism of vascular occlusion, regeneration of lung microvasculature may be a novel and effective therapeutic strategy for restoring pulmonary hemodynamics in patients with advanced PAH.

Our group has suggested that, as in systemic arterial beds, it may be possible to induce the regeneration of pulmonary microvessels in experimental models of lung vascular dis-

Original received October 18, 2004; revision received January 19, 2005; accepted January 20, 2005.

From the Terrence Donnelly Vascular Biology Laboratories, St Michael's Hospital and the McLaughlin Center for Molecular Medicine, University of Toronto, Canada.

Dr Stewart is a principal and CSO of Northern Therapeutics, and this work was funded in part by Northern Therapeutics.

Correspondence to Dr Duncan J. Stewart, Dexter Hung-Cho Man Chair and Director of the Division of Cardiology, University of Toronto, 30 Bond St, Suite 6-050k Queen Wing, Toronto, Ontario, Canada, M5B 1W8. E-mail stewartd@smh.toronto.on.ca

© 2005 American Heart Association, Inc.

Circulation Research is available at <http://www.circresaha.org>

DOI: 10.1161/01.RES.0000157672.70560.7b

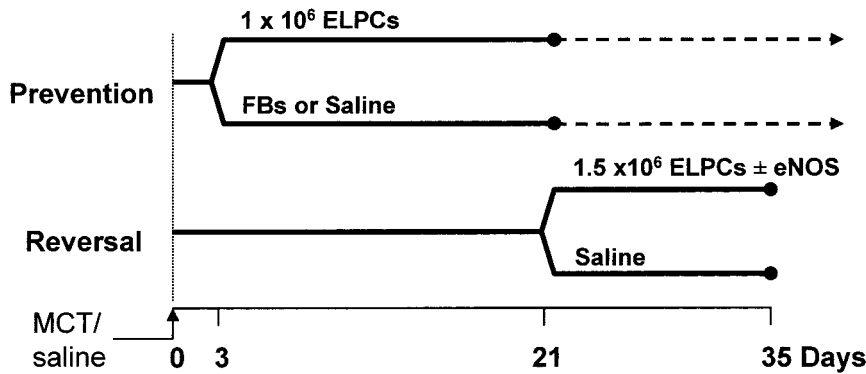


Figure 1. Experimental design of prevention and reversal protocols. In the prevention protocol, cell therapy was delivered 3 days after MCT injection and rats were followed for 21 days; control groups were compared with the ELPC-treated group. Persistence of therapeutic effect was investigated in separate groups of animals survived for longer periods (dotted lines). For reversal studies, rats were randomized to treatment groups at 21 days after MCT injection and initial hemodynamic measurements were made to confirm establishment of pulmonary arterial hypertension and to allow for paired comparisons within groups at end study 14 days later.

ease. We have shown that somatic cell-based gene therapy with endothelial NO-synthase (eNOS)¹³ or various angiogenic factors, including vascular endothelial growth factor (VEGF) and angiopoietin-1,^{14,15} can reduce monocrotaline (MCT)-induced PAH in prevention models, possibly by protecting against endothelial cell (EC) apoptosis or inducing microvascular angiogenesis. In addition, the administration of fibroblasts (FBs) transduced with eNOS resulted in significant improvement in right ventricular systolic pressure (RVSP) when delivered to rats with established PAH, associated with evidence of regeneration of the lung microcirculation (unpublished observations, 2004), and consistent with the now well-accepted role of eNOS and NO in angiogenesis.^{16–18} Recently, it has been recognized that circulating bone marrow-derived endothelial progenitor cells (EPCs) play an important role in repair of endothelial injury and participate directly in postnatal vasculogenesis and angiogenesis in systemic vascular beds.^{19,20} However, whether EPCs are involved in pulmonary endothelial repair and regeneration is not known, although it has recently been reported that circulating progenitor cells may be recruited to the remodeling adventitia in the bovine hypoxia model of PAH.²¹

Therefore, we studied the effect of bone marrow-derived endothelial-like progenitor cell (ELPC) transplantation in both the prevention and reversal models of PAH after the administration of MCT, which is well known to induce selective pulmonary endothelial injury in the rat. We now report that MCT-induced PAH could be completely prevented by treatment with syngeneic ELPCs. Moreover, delayed administration of ELPCs to animals 3 weeks after MCT injury prevented further progression of PAH, whereas the transplantation of eNOS-transduced ELPCs induced significant reversal of established disease to levels not different from saline-treated control animals. This was associated with evidence of restoration of distal arteriolar continuity and improved perfusion of alveolar capillaries in this model.

Materials and Methods

Cell Isolation and Culture

Skin biopsies were obtained from 21-day-old Fisher-344 rats (Charles River Co, St Constant, Quebec, Canada), and FBs were cultured using an explant technique. Cells were grown in Dulbecco Modified Eagle Media (DMEM) with 10% fetal bovine serum (FBS) and 2% penicillin/streptomycin (50 U/mL penicillin G; 50 μ g/mL streptomycin) in a humidified incubator (20% O₂, 5% CO₂ at 37°C), and used between passages 2 and 9.

Bone marrow (BM) was aspirated from the femurs of 21-day-old syngeneic Fisher-344 rats. Mononuclear cells (MNCs) were isolated by density gradient (Ficoll-Paque, Amersham) centrifugation at 400g for 30 minutes. BM-MNCs were resuspended in differential endothelial cell culture medium (EBM-2, Cambrex) with 10% FBS, 50 U/mL penicillin, 50 μ g/mL streptomycin, and 2 mmol/L L-glutamine (Invitrogen), plated on gelatin-coated tissue culture flasks and incubated at 37°C with 5% CO₂ for 7 to 10 days, to produce endothelial-like progenitor cells (ELPCs).

For immunocytochemistry, differentiated MNCs were subcultured on 4-well chamber slides (BD Bioscience), and fixed in 2% paraformaldehyde for 10 minutes. Cells were incubated overnight at 4°C with the following primary antibodies: rabbit anti-human Flk-1 (VEGF-R2; Alpha Diagnostic Inc; 1:200); mouse anti-human Tie-2 (Upstate Biotechnology Inc; 1:50), or rabbit anti-human von Willebrand factor (vWF, DAKO; 1:1000). Rabbit anti-mouse or goat anti-rabbit F(ab')₂ (Vector; 1:150) conjugated with FITC were used as secondary antibodies, as appropriate. Surface lectin staining was performed using fluorescently labeled UEA-1 Lectin (Sigma) at 10 μ g/mL. As well, the ability for live cells to take up fluorescently labeled acetylated-LDL (DiI-Ac-LDL; Molecular Probes) was assessed by incubation with DiI-Ac-LDL (10 μ g/mL) for 4 hours at 37°C. ToPro3 (1:1000; Molecular Probes) was used for nuclear counterstaining and images were captured by confocal microscopy (BioRad Radiance).

Transduction

The full-length coding sequence of human eNOS was generated as previously described,¹³ and ELPCs were transduced with human eNOS cloned into the pVax-1 plasmid vector using electroporation (MaxCyte) according to a protocol optimized by the manufacturer. The empty (null) pcDNA 3.1 vector was used as a control. After transfection, cells were replated and cultured for 24 hours, trypsinized (0.25% trypsin, 1% EDTA), washed, and resuspended in phosphate buffered saline (PBS), and then divided into aliquots of 500 000 cells/mL for injection. Western blot analysis revealed that electroporation resulted in peak human transgene expression at 72 hours, persisting for more than 1 week (data not shown).

Animal Models of PAH

Two complementary models of MCT-induced PAH were used in this study, as shown in Figure 1, to examine the effect of ELPC delivery on both prevention and reversal. All animal studies were conducted under protocols approved by the animal care committee at St Michael's Hospital and in accordance with guidelines from the Canadian Council of Animal Care.

Prevention Protocol

Cells were delivered via central venous injection 3 days after MCT, and the animals were euthanized at 21 days. Six-week-old Fisher-344 rats (160 to 180g) were given intraperitoneal (IP) injections of saline (control group, n=13) or 75 mg/kg of MCT (Aldrich Chemical Co). Three days later, MCT-treated animals were assigned to three experimental groups: no cell injection (MCT alone, n=15), or

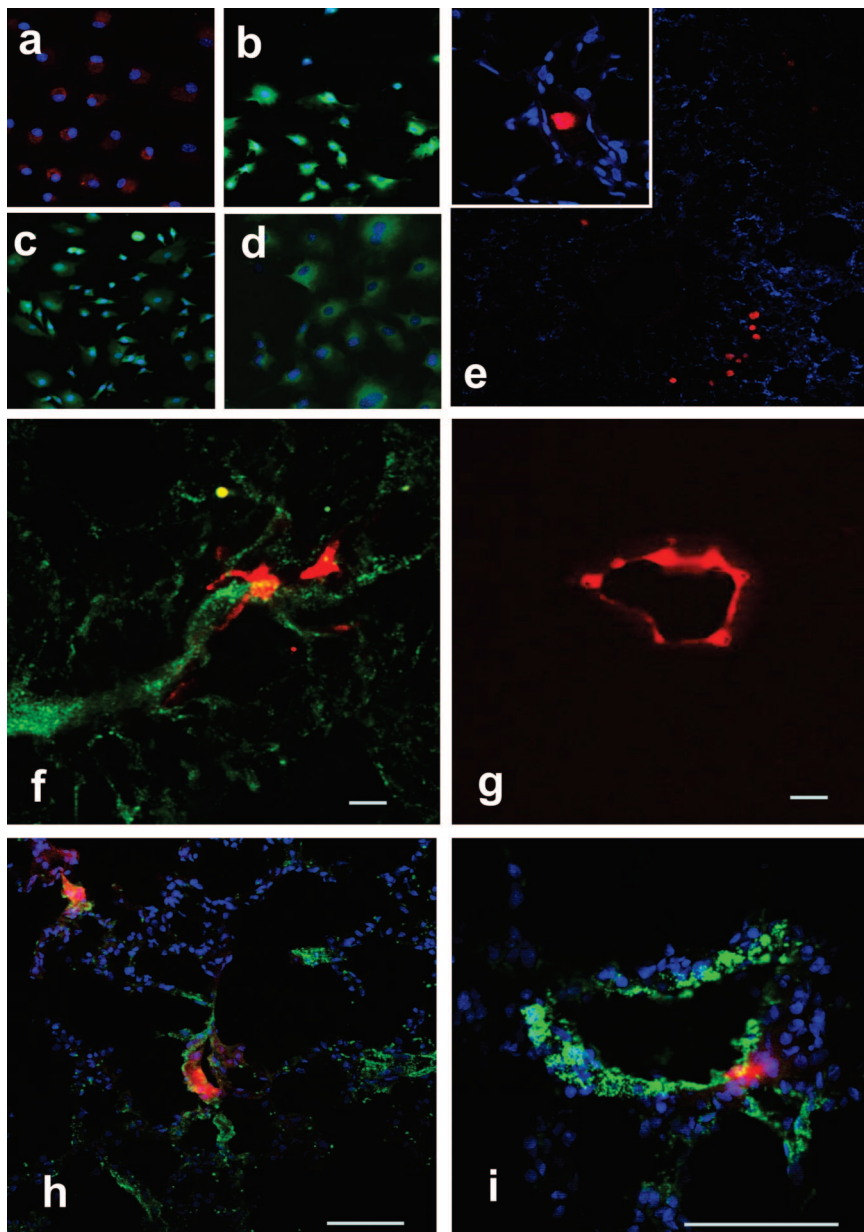


Figure 2. ELPC phenotype was characterized in vitro (a through d) by assessing Dil acetylated LDL uptake (red, a) and UEA-1 lectin surface staining (green, b), indirect immunofluorescence staining was performed to detect vWF (green, c) and Flk-1 (green, d) expression (blue, ToPro 3 nuclear counterstain in all panels). e through g, Fluorescently labeled (red) ELPCs were injected 3 days after MCT administration, and lungs were perfused with agarose containing fluorescent microspheres (green) just before harvest. At 15 minutes after injection, cells were trapped within distal arterioles (e). At later time points, injected cells were seen to engraft into the endothelial layer of distal precapillary arterioles as confirmed by fluorescent microangiography (green in f). In some areas, complete luminal incorporation was observed (g). h and i, Labeled ELPCs (red) delivered 21 days after MCT could be incorporating in precapillary and larger arterioles (vWF immunostaining in green; calibration bars=50 μ m).

1 million ELPCs (n=23) or FBs (n=10). For cell delivery, rats were anesthetized with an IP injection of xylazine (4.6 mg/kg) and ketamine (7 mg/kg), the left cervical area was shaved and cleaned with 70% ethanol, and the external jugular vein was catheterized with a polyethylene cannula flushed with heparinized saline (40 IU/mL). Twenty one days after MCT injection, the rats were reanesthetized, and a 3F Millar microtip catheter was inserted via the right external jugular vein and into the right ventricle to obtain measurements of right ventricular systolic pressure (RVSP; Biopac System, Acknowledge Software). The animals were then euthanized and the hearts and lungs harvested. The ratio of right to left ventricular plus septal weight (RV/LV) was determined as described previously.¹³ The left lung was inflated with OCT (Tissue-Tek) and cut into pieces that were fixed in a 4% paraformaldehyde/0.1% glutaraldehyde PBS solution for paraffin embedding and sectioning. The right lung was snap frozen in liquid nitrogen.

In a separate experiment, animals were treated with MCT and randomized at 3 days to receive either no cells (saline, n=13) or ELPCs (n=12) as described above and then followed for longer periods of time to establish the persistence of any therapeutic effect. The animals were monitored daily by experienced animal care

personnel in a blinded fashion and euthanized if predetermined criteria of significant morbidity were met (weight loss, hunched posture, poor coat appearance, conjunctival hemorrhage, and labored breathing). RVSP and RV/LV weight ratios were measured at the time of euthanasia as described above.

Reversal Protocol

In the reversal model, rats were injected with saline (Control, n=12) or MCT, and 21 days later, baseline RVSP was recorded as earlier to confirm the presence of PAH. Thereafter, polyethylene catheters were inserted into the left external jugular vein and tunneled subcutaneously to the intrascapular region, exiting through a small incision, and sealed to the external environment with a removable plug. All incisions were closed with 3-0 interrupted absorbable sutures. Rats were randomized to receive saline (MCT alone), ELPCs alone, or ELPCs transduced with human eNOS (n=19 to 23/group). Cells were given in three sequential injections of 5×10^5 over 3 days through the indwelling catheter (total dose= 1.5×10^6 cells). After the final cell injection, the indwelling catheter was removed, the left external jugular vein was ligated, and animals were

allowed to recover. Fourteen days later (35 days after MCT) RVSP was recorded, the animals were euthanized, and lung and heart tissues were collected for analyses as described.

Fluorescent Microangiography

In a subset of animals, a catheter was inserted into the pulmonary artery immediately after euthanasia and the lungs flushed with heparinized PBS at 37°C, immediately followed by perfusion with a warmed (45°C) solution of 1% low melting point agarose (Sigma) containing 0.2 μm yellow-green fluorescent microspheres (505/515 nm peak excitation and emission, Molecular Probes) as described in detail in the expanded Materials and Methods section in the online data supplement available at <http://circres.ahajournals.org>.

Engraftment of ELPCs

In separate experiments, ELPCs were loaded with the vital cytoplasmic fluorescent label, CMTMR (Molecular Probes). Before transplantation, subconfluent cultures of ELPCs were incubated for 40 minutes with 10 $\mu\text{mol/L}$ CMTMR, and 1×10^6 labeled cells were injected into the pulmonary circulation of normal rats at 3 or 21 days after MCT injection via the external jugular vein as described. Lungs or kidneys were harvested at various time points (10 minutes to 3 weeks) after cell delivery and examined by confocal fluorescent microscopy. Quantitation of cell number was performed as previously described.¹³ In some cases, the lungs were also subjected to fluorescent microangiography and confocal images were captured by optical sectioning as described.

Arteriolar Muscularization

The degree of muscularization of small arterioles was assessed in 5 μm lung cryosections immunostained for von Willebrand factor (vWF) and α -smooth muscle actin (α -SM-actin) as described in the online data supplement.

Statistical Analysis

Data are presented as mean \pm SEM. Differences between groups were assessed by using analysis of variance (ANOVA), followed by post hoc comparisons using an unpaired *t* test as appropriate. Differences within groups between the 21- and 35-day time points were assessed using a paired *t* test. Significance of differences for survival data were determined using the Kaplan-Meier analysis. A value of $P < 0.05$ was considered statistically significant.

Results

In Vitro Characterization of ELPCs

After 7 to 10 days of culture in endothelial growth medium, BM-MNCs demonstrated a cobblestone appearance typical for endothelial cells and exhibited positivity for a panel of EC markers, including DiI acLDL, UEA-1 lectin staining, and immunostaining for vWF, and Flk-1 varying from 65% to 83% (Figure 2).

Engraftment of Fluorescently-Labeled ELPCs

CMTMR-labeled ELPCs were injected into the pulmonary circulation 3 days after administration of MCT. Fifteen minutes after delivery, labeled ELPCs were seen distributed throughout the lung (Figure 2e), nearly exclusively within small precapillary arterioles (insert). Seven days after cell injection, fluorescently-tagged ELPCs were seen surrounding and engrafting distal arterioles (Figure 2f) and on occasions integrating into, and regenerating, the endothelium of larger arterioles (Figure 2g). After the first 3 days, the number of engrafted ELPCs was fairly constant up to 3 weeks (see online Figure WS-2, in the online data supplement). Similar

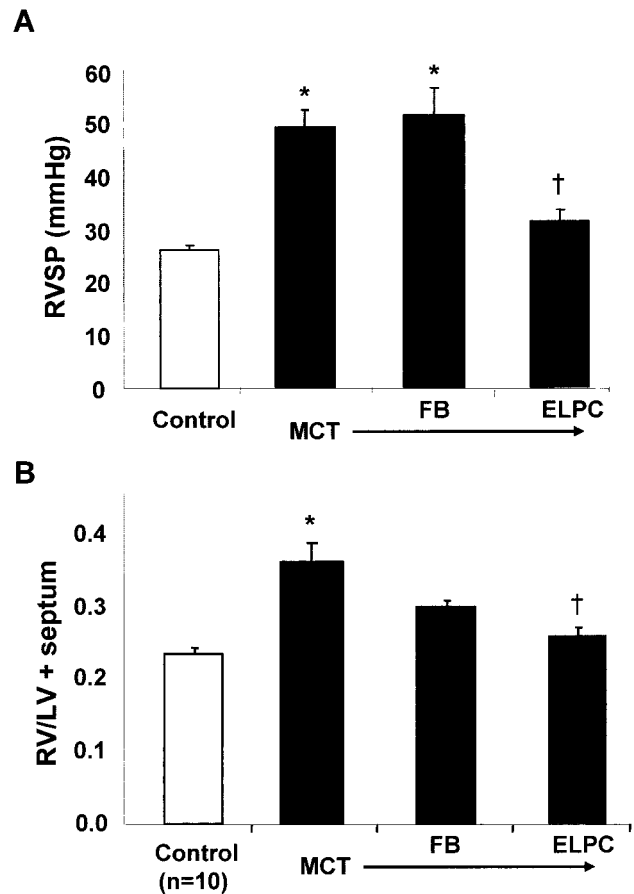


Figure 3. Effect of early ELPC injection (prevention protocol) on right ventricular systolic pressure (RVSP) and the ratio of right ventricular to left ventricular weight (RV/LV) at end-study (day 21). In rats receiving fibroblasts ($n=10$), there was a marked increase in RVSP and a slight increase in the RV/LV ratio. However, the ELPC-treated rats ($n=23$) exhibited a significantly lower RVSP than the fibroblast group ($P < 0.001$) with no significant increase in the RV/LV ratio. Data from age-matched normal rats are presented for comparison. * $P < 0.001$ vs control, † $P < 0.001$ vs MCT

results were obtained when labeled ELPCs were delivered 21 days after MCT (Figure 2h and 2i).

ELPC Administration in the Prevention Model

RVSP was significantly increased at day 21 after MCT compared with saline-treated control rats (48 ± 3 versus 26 ± 0.9 mm Hg, $P < 0.001$; Figure 3A). Administration of somatic cells (ie, skin FBs) had no protective effect (RVSP 51 ± 5 mm Hg), whereas the delivery of syngeneic ELPCs nearly completely prevented the rise in pulmonary systolic pressures at 3 weeks after MCT (32 ± 1 mm Hg, $P < 0.001$ versus MCT alone). Similarly, right ventricular hypertrophy as measured by the ratio of RV/LV weight ratio was increased in animals receiving MCT alone (0.36 ± 0.02) or MCT with FBs (0.30 ± 0.01 ; Figure 3B). In contrast, the delivery of bone marrow-derived ELPCs significantly reduced right ventricular hypertrophy (0.26 ± 0.013 , $P < 0.01$ versus MCT) to a level not significantly different from saline-treated control animals (0.23 ± 0.01).

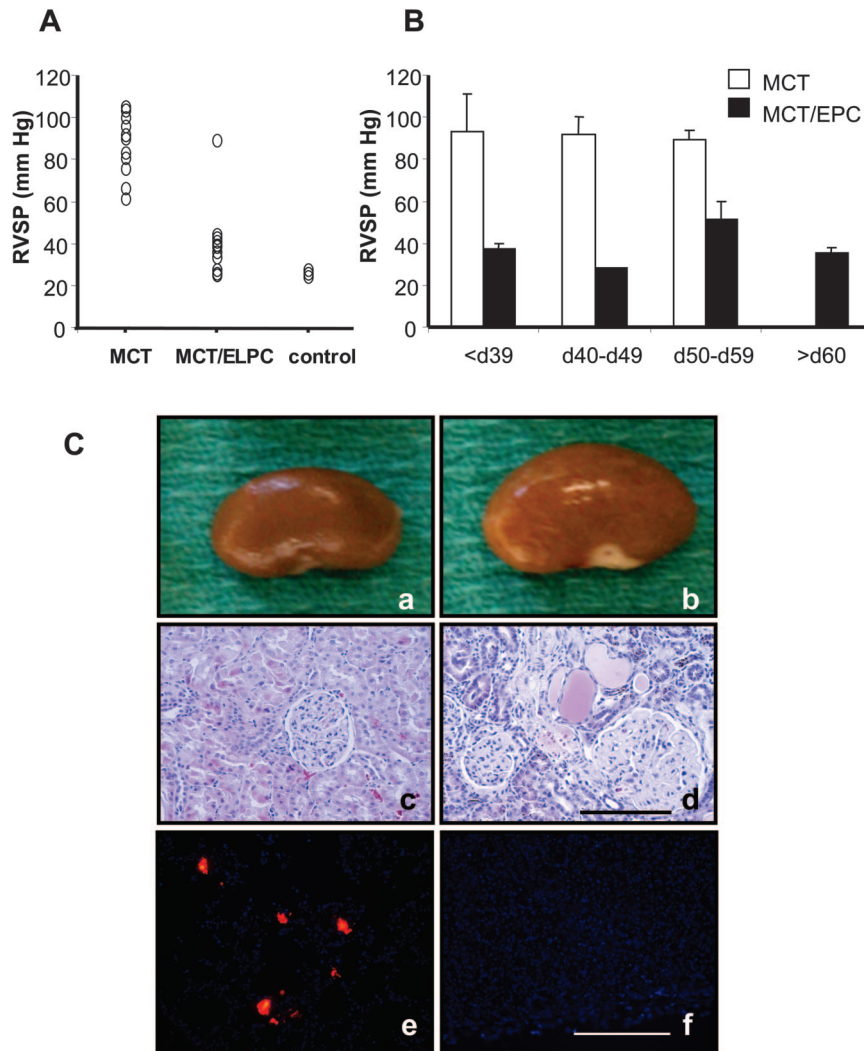


Figure 4. Persistence of effect was examined in a separate prevention study over a longer time period. RVSP was measured and animals euthanized on the development of predetermined signs of significant morbidity. ELPC group ($n=12$) exhibited near normal levels of RVSP at euthanasia with only one outlier; in contrast, RVSP in rats injected with fibroblasts ($n=13$) was markedly elevated (A, $P=0.001$, vs ELPC group). When analyzed according to time of euthanasia, there was no trend toward an increased RVSP in the ELPC-treated group even at more than 60 days (B). Kidneys (C) from MCT-ELPC-treated rats euthanized at later time points were enlarged with an irregular capsular surface (b), a marked contrast to those from control rats (a). Histological examination of kidneys from MCT-ELPC-treated rats (d) revealed changes consistent with end stage renal disease including glomerular enlargement, mesangial cell loss, and tubule hyalinization. Normal kidney histology is shown for comparison (c). In contrast to the lung (e), no fluorescently-labeled ELPCs were seen in the kidneys of MCT treated rats 20 minutes after injection (f) (calibration bars= $100\ \mu\text{m}$) or at later time points (data not shown).

Persistence of Protective Effects of ELPCs

At the time of euthanasia, RVSP was again markedly elevated in animals receiving MCT alone (Figure 4A), whereas with the exception of one animal, ELPC-treated rats exhibited near normal values of pulmonary systolic pressure. Moreover, there was no tendency for RVSP to increase in the ELPC-treated group over more than 60 days (Figure 4B). Nonetheless, despite this dramatic hemodynamic improvement, there was only a modest difference in "survival" between the groups ($P=0.08$), suggesting that the apparent morbidity observed in ELPC-treated animals might be caused by extrapulmonary MCT toxicity. Indeed, necropsy studies in the longest surviving MCT-treated rats revealed markedly enlarged kidneys that exhibited severe histological abnormalities of glomerular and tubular structure consistent with end-stage renal disease in both groups (Figure 4Ca through 4Cd). Unlike the lung, no renal engraftment of ELPCs was seen either immediately or 3 days after cell delivery (Figure 4Ce and 4Cf)

Effect of ELPC Transplantation in the Reversal Model

At 3 weeks after MCT injection, animals assigned to the three treatment groups exhibited similar increases in RVSP com-

pared with saline controls (Figure 5A) and comparable to that of the MCT alone group in the prevention protocol. Two weeks later, RVSP had progressed in the MCT animals treated with saline. The delivery of nontransduced ELPCs prevented the further progression of PAH from day 21 (43 ± 4 mm Hg) to day 35 (36 ± 4 mm Hg); however, only animals receiving eNOS-transduced ELPCs demonstrated significant improvement in RVSP at day 35 (31 ± 2 mm Hg) compared with day 21 (50 ± 3 mm Hg, $P<0.005$; Figure 6A). Of note, transgene expression was transient and persisted for only ≈ 1 week after electroporation (online Figure WS-2). The ratio of RV to LV and septal weight was significantly increased in the MCT-treated rats receiving only saline, whereas both ELPC-treated groups displayed significant reductions compared with control rats (Figure 5B). Similarly, the effects of MCT on the expression of VEGF and markers of endothelial activation (E- and P-Selectin) were normalized by administration of eNOS-transduced ELPCs (online Figure WS-1).

Effects of ELPCs on Fluorescent Microangiography

In normal lungs, microangiography revealed an even filling of the distal arteriolar bed with a homogeneous pattern of

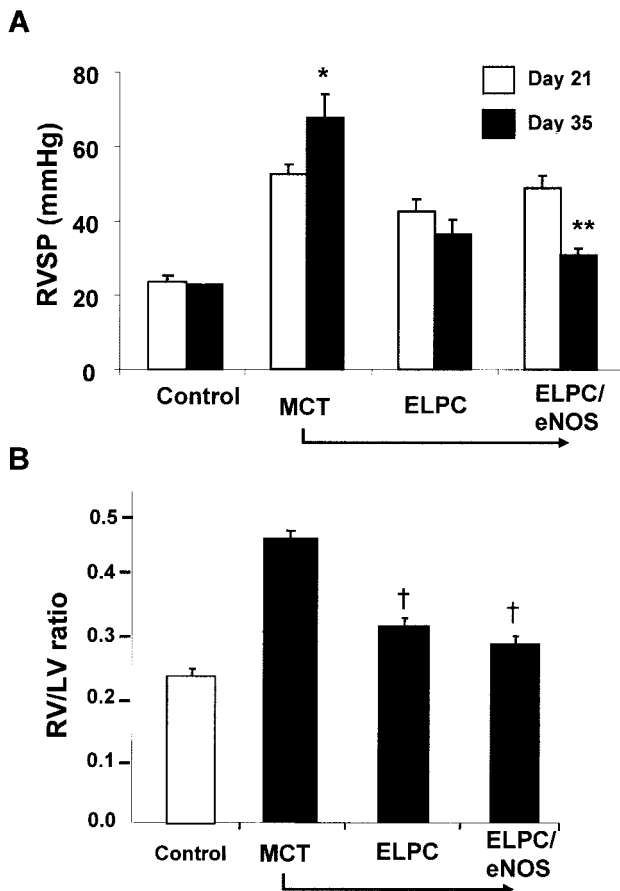


Figure 5. In reversal studies, RVSP (A) was measured at 21 days after MCT and again 14 days after cell therapy (day 35) in the same animals. In MCT-saline-injected rats, a significant progression in RVSP was observed, ELPC treatment inhibited this progression, and eNOS transduced ELPC treatment resulted in reversal of PAH with significantly lower RVSP values at day 35. Right ventricular hypertrophy was assessed by the RV/LV weight ratio determined at time of euthanization (B). Rats receiving MCT alone showed a significant increase in the RV/LV ratio at day 35 after MCT injection when compared with controls; in contrast, rats receiving eNOS-ELPCs or ELPCs alone had markedly reduced hypertrophy. * $P < 0.05$ vs day 21; ** $P < 0.005$ vs day 21; † $P < 0.001$ vs MCT.

capillary perfusion (Figure 6Aa). Immunostaining with an antibody directed to α -SM actin showed minimal muscularization of the distal arterioles in normal lungs. In contrast, 3 or 5 weeks after MCT-induced lung injury (Figure 6Ab and Ad, respectively), the distal arteriolar bed showed significant narrowing of distal arterioles with widespread capillary occlusion and evidence of increased distal muscularization. In animals receiving ELPCs 3 days after MCT, there was a marked improvement in the appearance of the lung microvasculature, with preservation of arteriolar continuity and enhanced capillary perfusion (Figure 6Ac). When ELPCs alone were administered 3 weeks after MCT, only modest improvement in capillary perfusion was seen (Figure 6Ae) with persistent distal muscularization. Only eNOS-transduced ELPCs restored a more normal appearance of the lung circulation in the reversal model (Figure 6Af). These observations were confirmed by quantification of microvascular perfusion as shown in Figure 6B ($n=6$ to 7/group).

Arteriolar Muscularization

In normal lungs, arterioles of $<30 \mu\text{m}$ showed infrequent muscularization with only 14% demonstrating partial muscularization (PM) and no vessels exhibiting full muscularization (FM). In contrast, 35 days after MCT there was a significantly higher proportion of muscularized arterioles (Figure 6C). Treatment with eNOS-transduced progenitor cells reduced arteriolar muscularization, whereas nontransduced ELPCs did not, although there was an increase overall in nonmuscularized vessels in both ELPC-treated groups compared with MCT alone.

Survival Analysis

In one experiment, only one animal in the MCT-saline group survived to the predefined study end point at 35 days after MCT, and therefore, these data were used for survival analysis only (Figure 7). The injection of ELPCs transduced with eNOS nearly completely prevented MCT-induced mortality with all but one animal surviving to end-study ($P=0.02$ versus MCT alone), whereas delivery of nontransduced ELPCs produced an intermediate survival that was not significantly different from MCT alone. However, when the survival analysis was performed including all 63 animals randomized in the reversal protocol, this trend persisted with the survival benefit in MCT-treated animals receiving nontransduced ELPC now reaching statistical significance ($P=0.037$ versus MCT alone).

Discussion

We now report that bone marrow-derived ELPCs engrafted the MCT-injured lung and incorporated into the pulmonary microvasculature, resulting in near complete prevention of PAH when delivered into the pulmonary circulation within 3 days of MCT injury. Although nontransduced ELPCs also prevented further increases in RVSP when injected 3 weeks after MCT-induced lung injury, only eNOS-transduced cells resulted in normalization of pulmonary hemodynamics in animals with established PAH, and this effect was associated with a significant survival benefit. Progenitor cell therapy also resulted in marked improvement in the pulmonary microvascular architecture and alveolar capillary perfusion in MCT-treated animals, which could in part be attributed to repair and regeneration of lung microvascular endothelium.

These findings may have important implications both with respect to the mechanisms underlying the development of PAH in this model, and for potential therapeutic strategies for the treatment of this disease. The present data suggest that loss of arteriolar continuity at the precapillary level may be a relatively early and widespread phenomenon, and may contribute directly to the increase in pulmonary vascular resistance by resulting in loss of pulmonary microcirculation. Fluorescent imaging of the microcirculation in thick sections revealed widespread discontinuity of the pulmonary arteriolar bed as early as 3 weeks after MCT-induced injury, mainly localized to the level of the precapillary (intraductal) arteriole. Of interest, despite the well-known differences in lung pathology, distal arteriolar occlusions have also been observed in lung tissue from patients with advanced idiopathic

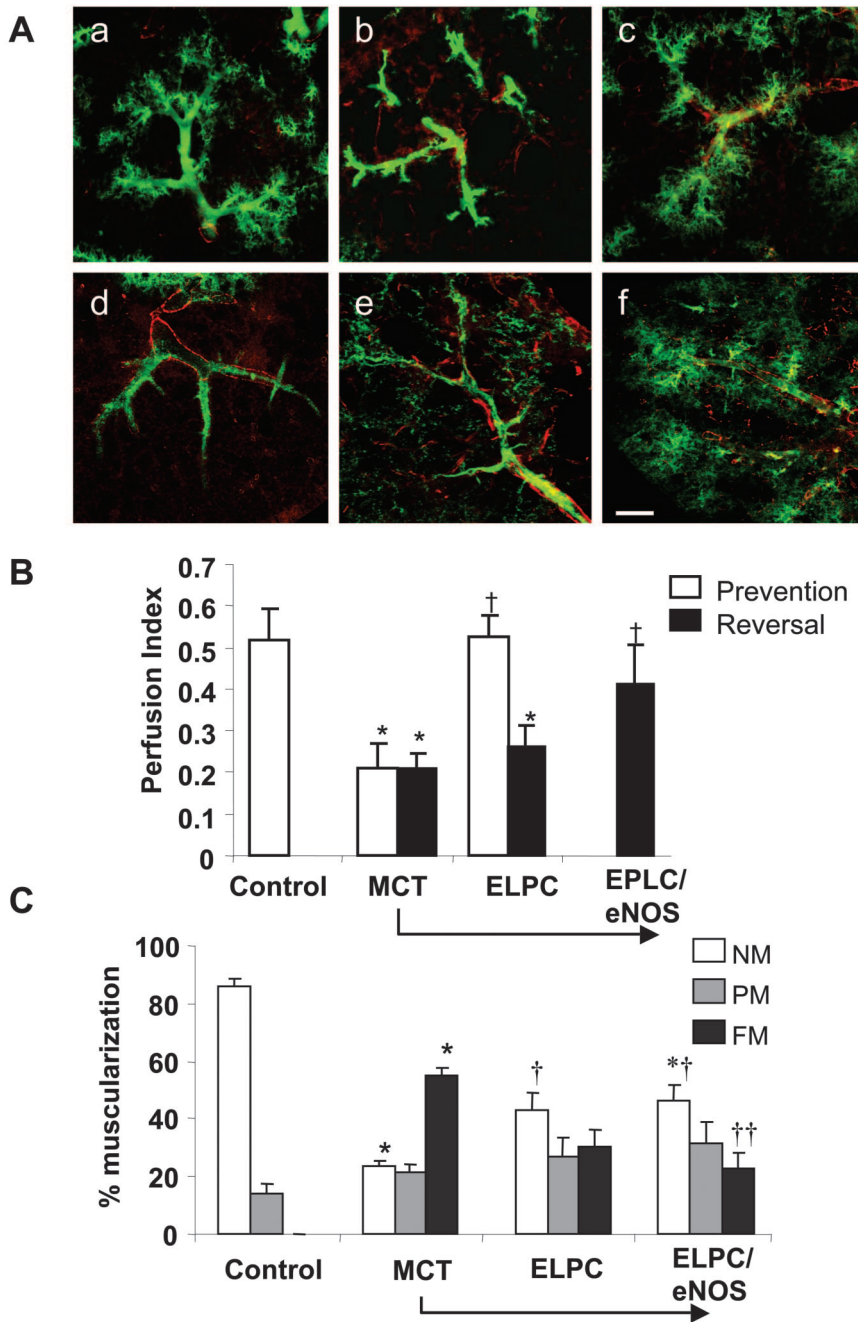


Figure 6. Representative confocal projection images of lung sections (A) perfused with fluorescent microspheres (green) suspended in agarose (ie, fluorescent microangiography) and immunostained for α -smooth muscle actin (red). Normal filling of the microvasculature was observed in control rats (a), whereas rats treated with MCT showed a marked loss of microvascular perfusion and widespread precapillary occlusion 21 (b) and 35 (d) days after MCT injection. In the prevention model, animals receiving ELPCs displayed improved microvascular perfusion and preserved continuity of the distal vasculature (c). In the reversal model, eNOS-transduced ELPCs dramatically improved the appearance of the pulmonary microvasculature (f), whereas progenitor cells alone resulted in more modest increases in perfusion and little noticeable reduction in arteriolar muscularization (e, calibration bars=100 μ m). Summary data for pulmonary microvascular perfusion (B; 6 to 7 animal/group) for animals treated in the prevention (open bars) and reversal (closed bars) protocols. Proportion of small pulmonary arterioles (C; <30 μ m) that are nonmuscularized (NM), partially (PM), or fully muscularized (FM) in the various treatment groups of the reversal protocol (9 to 13 animals per group). * P <0.05 vs control; † P <0.05 vs MCT-saline

PAH,⁷ although the mechanism of arteriolar occlusion in patients with PAH is still a matter of debate.

The observation that administration of ELPCs soon after MCT-induced lung injury protected against the development of PAH favors the concept that endothelial damage plays an important role in the pathogenesis of PAH in this model by contributing to microvascular loss. It is likely that engraftment of ELPCs at the level of the distal arteriolar bed reduced the consequences of MCT damage either by contributing to endothelial repair directly¹⁹ or indirectly by release of paracrine signals.²² This interpretation is supported by fluorescent microangiography showing that the pruning and occlusion of precapillary arterioles induced by MCT was nearly completely obviated by the

administration of ELPCs. This effect was dependent on the delivery of “regenerative” cells, because injection of a somatic cell line, ie, skin FBs, had no effect on microvascular structure or function. Of interest, the protective effect of ELPCs appeared to persist as long as it was possible to follow the animals. Indeed, the prevention of MCT-induced vascular damage in the lung unmasked profound renal toxicity, which had been previously recognized in the reports that first characterized the toxicity of MCT.^{23,24} This additional toxic effect of MCT clearly represents a significant limitation for studies of long-term survival after lung-specific therapy of PAH in this model.

The efficacy of nontransduced ELPCs in the prevention of PAH in this study are in contrast with a recent report using

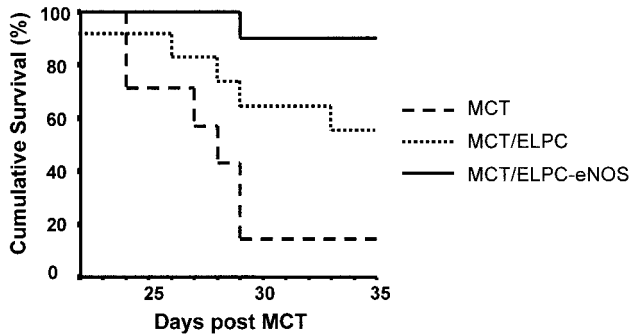


Figure 7. Survival to 35 days was analyzed in a separate reversal study. Kaplan-Meier analysis demonstrated that treatment with eNOS transduced ELPCs 21 days after MCT injection produced enhanced survival as compared with the MCT alone group ($P=0.02$). Although animals receiving ELPCs alone showed an intermediate response, the improvement was not statistically significant in this cohort.

human umbilical cord progenitor cells injected into immunodeficient rats,²⁵ in which significant prevention of MCT-induced PAH was seen only with adrenomedullin-transfected cells, with little or no benefit using ELPCs alone. This discrepancy may be related to differences in the source of progenitor cells (ie, cord blood versus bone marrow) or to species-specific factors that may limit the regenerative effects of human cells in the rat model.²⁶ Nonetheless, the Nagaya report confirms a number of previous reports from our group showing the efficacy of cell-based gene therapy in the “prevention” MCT model using a variety of somatic cell types and therapeutic transgenes,^{14,15} including eNOS.¹³

However, prevention of PAH is not a clinically relevant therapeutic target because patients only present once this disease is already in its advanced stages. In the setting of established PAH, although ELPCs alone reduced progression of MCT-induced PAH, they did not produce significant improvement in pulmonary systolic pressures over the subsequent 2-week interval. In contrast, the delivery of ELPCs transduced with eNOS resulted in near normalization of right ventricular systolic pressures, which was associated with marked improvement of microvascular architecture and alveolar capillary perfusion. The added benefit of eNOS gene transfer is consistent with a growing body of literature that supports an important role for endothelium-derived NO in angiogenesis and vascular regeneration, both acting as a downstream mediator for a variety of classical angiogenic growth factors,^{16,17,27} as well as by inducing an angiogenic profile of gene expression.^{28,29} Of interest, our group has identified a previously unsuspected role for eNOS in the development of the fetal lung vasculature and in the maturation of the airway epithelial cells.²⁹ Specifically, eNOS appears to be essential for the establishment of arteriolar-capillary continuity in the mid to late gestational fetal lung circulation, and eNOS-deficient pups exhibit pathological features that are nearly identical to alveolar capillary dysplasia,^{30–32} a pernicious form of persistent pulmonary hypertension of the newborn that is nearly always fatal. Moreover, we have demonstrated that cell-based gene transfer of eNOS resulted in partial reversal of MCT-induced PAH even using a somatic (FB) cell line (manuscript in preparation), although

the magnitude of benefit was less than that seen with eNOS-transduced ELPCs. Together, these data point to a critical role for eNOS in control of vascular growth and the development of a competent pulmonary circulation both during fetal development as well as in arteriolar regeneration in postnatal MCT-injured lung.

The present results provide further support for the view that microvascular degeneration at the critical precapillary level may play an important role in the development of PAH by leading to the exclusion of large portions of the pulmonary microvasculature from the pulmonary circulation. Moreover, they show for the first time that eNOS-transduced ELPCs can dramatically improve pulmonary hemodynamics and survival in animals with established PAH, while restoring the continuity of the distal arteriolar bed. These data have important implications for the therapy of this lethal disease and support the exploration of regenerative cell-based gene strategies for the treatment of patients with severe refractory PAH for whom therapeutic options are very limited and the prognosis is poor.

Acknowledgments

The study was supported by research grants from the Canadian Institutes for Health Research (MPO-57726) and by Northern Therapeutics Inc. D.J.S. is a member of the Richard Lewar Center of Excellence. The authors would like to acknowledge the outstanding technical assistance of Robin N.N. Han, Douglas Ng, Malcolm Robb, Judy Trogradis, and Danlin Jia.

References

1. Archer S, Rich S. Primary pulmonary hypertension: a vascular biology and translational research “Work in progress.” *Circulation*. 2000;102:2781–2791.
2. Deng Z, Morse JH, Slager SL, Cuervo N, Moore KJ, Venetos G, Kalachikov S, Cayanis E, Fischer SG, Barst RJ, Hodge SE, Knowles JA. Familial primary pulmonary hypertension (gene PPH1) is caused by mutations in the bone morphogenetic protein receptor-II gene. *Am J Hum Genet*. 2000;67:737–744.
3. Humbert M, Deng Z, Simonneau G, Barst RJ, Sitbon O, Wolf M, Cuervo N, Moore KJ, Hodge SE, Knowles JA, Morse JH. BMPR2 germline mutations in pulmonary hypertension associated with fenfluramine derivatives. *Eur Respir J*. 2002;20:518–523.
4. Lane KB, Machado RD, Pauciuolo MW, Thomson JR, Phillips JA, III, Loyd JE, Nichols WC, Trembath RC. Heterozygous germline mutations in BMPR2, encoding a TGF-beta receptor, cause familial primary pulmonary hypertension: the International PPH Consortium. *Nat Genet*. 2000;26:81–84.
5. Morrell NW, Yang X, Upton PD, Jourdan KB, Morgan N, Sheares KK, Trembath RC. Altered growth responses of pulmonary artery smooth muscle cells from patients with primary pulmonary hypertension to transforming growth factor- β 1 and bone morphogenetic proteins. *Circulation*. 2001;104:790–795.
6. Morse JH, Deng Z, Knowles JA. Genetic aspects of pulmonary arterial hypertension. *Ann Med*. 2001;33:596–603.
7. Cool CD, Stewart JS, Weraheha P, Miller GJ, Williams RL, Voelkel NF, Tuder RM. Three-dimensional reconstruction of pulmonary arteries in plexiform pulmonary hypertension using cell-specific markers: evidence for a dynamic and heterogeneous process of pulmonary endothelial cell growth. *Am J Pathol*. 1999;155:411–419.
8. Voelkel NF, Cool C. Pathology of pulmonary hypertension. *Cardiol Clin*. 2004;22:343–351.
9. Taraseviciene-Stewart L, Kasahara Y, Alger L, Hirth P, Mc MG, Waltenberger J, Voelkel NF, Tuder RM. Inhibition of the VEGF receptor 2 combined with chronic hypoxia causes cell death-dependent pulmonary endothelial cell proliferation and severe pulmonary hypertension. *FASEB J*. 2001;15:427–438.

10. Holash J, Wiegand SJ, Yancopoulos GD. New model of tumor angiogenesis: dynamic balance between vessel regression and growth mediated by angiopoietins and VEGF. *Oncogene*. 1999;18:5356–5362.
11. Golpon HA, Fadok VA, Taraseviciene-Stewart L, Scerbavicius R, Sauer C, Welte T, Henson PM, Voelkel NF. Life after corpse engulfment: phagocytosis of apoptotic cells leads to VEGF secretion and cell growth. *FASEB J*. 2004;18:1716–1718.
12. Voelkel NF, Cool C, Taraseviciene-Stewart L, Geraci MW, Yeager M, Bull T, Kasper M, Tuder RM. Janus face of vascular endothelial growth factor: the obligatory survival factor for lung vascular endothelium controls precapillary artery remodeling in severe pulmonary hypertension. *Crit Care Med*. 2002;30:S251–S256.
13. Campbell AI, Kuliszewski MA, Stewart DJ. Cell-based gene transfer to the pulmonary vasculature: endothelial nitric oxide synthase overexpression inhibits monocrotaline-induced pulmonary hypertension. *Am J Respir Cell Mol Biol*. 1999;21:567–575.
14. Campbell AI, Zhao Y, Sandhu R, Stewart DJ. Cell-based gene transfer of vascular endothelial growth factor attenuates monocrotaline-induced pulmonary hypertension. *Circulation*. 2001;104:2242–2248.
15. Zhao YD, Campbell AI, Robb M, Ng D, Stewart DJ. Protective role of angiopoietin-1 in experimental pulmonary hypertension. *Circ Res*. 2003;92:984–991.
16. Babaei S, Stewart DJ. Overexpression of endothelial NO synthase induces angiogenesis in a co-culture model. *Cardiovasc Res*. 2002;55:190–200.
17. Cooke JP. NO and angiogenesis. *Atheroscler Suppl*. 2003;4:53–60.
18. Ziche M, Morbidelli L, Choudhuri R, Zhang HT, Donnini S, Granger HJ, Bicknell R. Nitric oxide synthase lies downstream from vascular endothelial growth factor-induced but not basic fibroblast growth factor-induced angiogenesis. *J Clin Invest*. 1997;99:2625–2634.
19. Asahara T, Kawamoto A. Endothelial progenitor cells for postnatal vasculogenesis. *Am J Physiol Cell Physiol*. 2004;287:C572–C579.
20. Luttun A, Carmeliet G, Carmeliet P. Vascular progenitors: from biology to treatment. *Trends Cardiovasc Med*. 2002;12:88–96.
21. Davie NJ, Crossno JT, Jr., Frid MG, Hofmeister SE, Reeves JT, Hyde DM, Carpenter TC, Brunetti JA, McNiece IK, Stenmark KR. Hypoxia-induced pulmonary artery adventitial remodeling and neovascularization: contribution of progenitor cells. *Am J Physiol Lung Cell Mol Physiol*. 2004;286:L668–L678.
22. Rafii S, Meeus S, Dias S, Hattori K, Heissig B, Shmelkov S, Rafii D, Lyden D. Contribution of marrow-derived progenitors to vascular and cardiac regeneration. *Semin Cell Dev Biol*. 2002;13:61–67.
23. Carstens LA, Allen JR. Arterial degeneration and glomerular hyalinization in the kidney of monocrotaline-intoxicated rats. *Am J Pathol*. 1970;60:75–92.
24. Kurozumi T, Tanaka K, Kido M, Shoyama Y. Monocrotaline-induced renal lesions. *Exp Mol Pathol*. 1983;39:377–386.
25. Nagaya N, Kangawa K, Kanda M, Uematsu M, Horio T, Fukuyama N, Hino J, Harada-Shiba M, Okumura H, Tabata Y, Mochizuki N, Chiba Y, Nishioka K, Miyatake K, Asahara T, Hara H, Mori H. Hybrid cell-gene therapy for pulmonary hypertension based on phagocytosing action of endothelial progenitor cells. *Circulation*. 2003;108:889–895.
26. Stewart DJ, Zhao YD, Courtman DW. Cell therapy for pulmonary hypertension: what is the true potential of endothelial progenitor cells? *Circulation*. 2004;109:e172–e173.
27. Morbidelli L, Donnini S, Ziche M. Role of nitric oxide in tumor angiogenesis. *Cancer Treat Res*. 2004;117:155–167.
28. Namba T, Koike H, Murakami K, Aoki M, Makino H, Hashiya N, Ogihara T, Kaneda Y, Kohno M, Morishita R. Angiogenesis induced by endothelial nitric oxide synthase gene through vascular endothelial growth factor expression in a rat hindlimb ischemia model. *Circulation*. 2003;108:2250–2257.
29. Han RN, Babaei S, Robb M, Lee T, Ridsdale R, Ackerley C, Post M, Stewart DJ. Defective lung vascular development and fatal respiratory distress in endothelial NO synthase-deficient mice: a model of alveolar capillary dysplasia? *Circ Res*. 2004;94:1115–1123.
30. Cai J, Ahmad S, Jiang WG, Huang J, Kontos CD, Boulton M, Ahmed A. Activation of vascular endothelial growth factor receptor-1 sustains angiogenesis and Bcl-2 expression via the phosphatidylinositol 3-kinase pathway in endothelial cells. *Diabetes*. 2003;52:2959–2968.
31. Gutierrez C, Rodriguez A, Palenzuela S, Forteza C, Rossello JL. Congenital misalignment of pulmonary veins with alveolar capillary dysplasia causing persistent neonatal pulmonary hypertension: report of two affected siblings. *Pediatr Dev Pathol*. 2000;3:271–276.
32. Tibballs J, Chow CW. Incidence of alveolar capillary dysplasia in severe idiopathic persistent pulmonary hypertension of the newborn. *J Paediatr Child Health*. 2002;38:397–400.